4
Results

4.1.
Density and specific gravity

Density and specific gravity of samples, from inner, outer, bottom and middle sections of the culm are presented on Table 6. Bottom SG was around 0,63 – 0,64 while the middle one was between 0,74 and 0,86. Values allow plotting SG, as suggested by Ghavami, 1995 relation to the position along the culm length for both inner and outer sides.

Specimen	mass [gr]	sample's dimensions			density [gr/cm³]	Especific Gravity
		lenght [mm]	wide [mm]	thick [mm]		
1 Middle-Outer	26,304	227	36,76	3,67	0,86	0,86
2 Bottom-Outer	12,918	229	34,84	2,58	0,63	0,63
3 Middle-Inner	27,116	228	40,78	3,94	0,74	0,74
4 Bottom-Inner	16,333	225	39,095	2,91	0,64	0,64

Table 6 Density and specific gravity for bottom and middle segments.

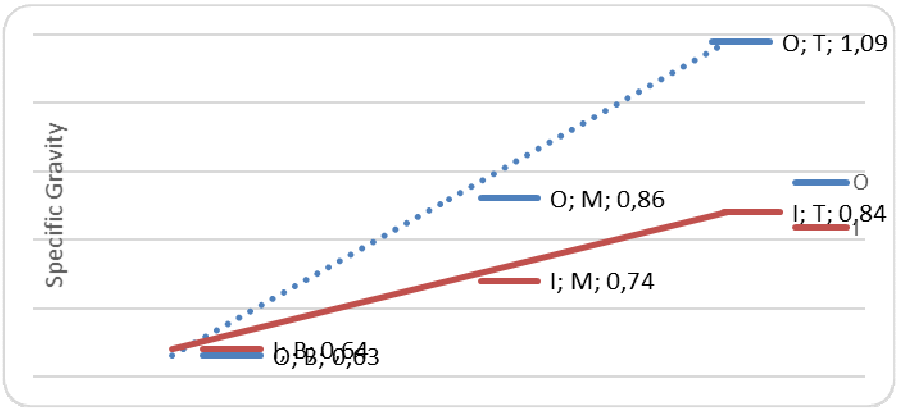

Figure 31 Specific Gravity of inner and outer segments along the culm length.

4.2. Moisture

For moisture calculations, five samples were taken from different locations along the culm, results are presented below on Table 7. The average value of moisture was 11,11%.

Sample	m_0 [gr]	m [gr]	Humidity [%]
1	16,85	15,12	11,44%
2	13,61	12,23	11,28%
3	21,17	19,06	11,07%
4	9,42	8,47	11,22%
5	7,66	6,93	10,53%
Average			11,11%

Table 7 Moisture of bamboo used for test specimens and beams.

4.3. Roughness

Results for roughness measurements are shown in Figure 33. The range of readings were 9,55 mm for X-axis and 168,18 µm for Y-axis. Results had an outstanding accuracy as the machine has a precision ranges of µm, however, the bamboo roughness values were around of 40,78 µm shown in the Figure 33.

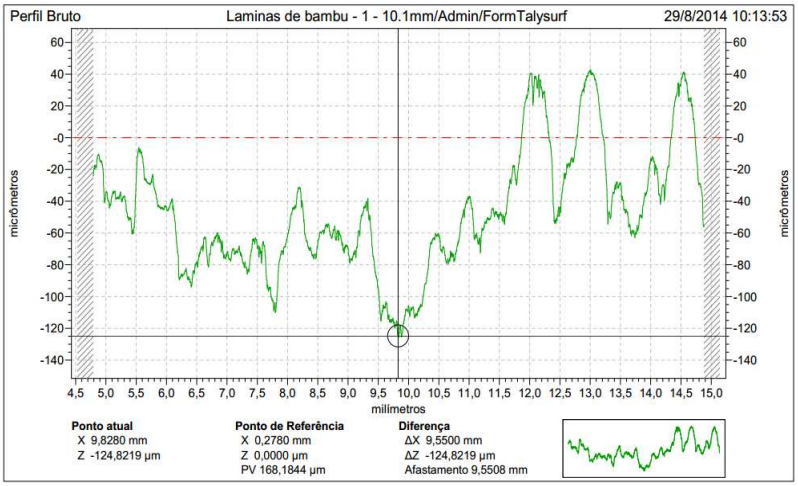

Figure 32 Profile of final polished bamboo laminas surface.

The curve shown in the lower right corner of Figure 33 provides the surface profile of the segment shown in Figure 34. This was done, mainly to verify an

acceptable roughness value to allow optimal adhesion between layers, despite it looks considerably flat at first glance. Surfaces were found to be sufficiently flat and smooth to ensure adherence, when compared with benchmarks from other laminated bamboo studies.

Figure 33 Surfaces of final layers used to obtain test specimens and assemble beams.

4.4. Test specimens analysis

The measurements presented were obtained using clip gages for both tensile and shear tests, and running three of them equipped with strain gages to check values. The variability between results is attributed to the differences in testing parameters, as summarized previously, and the multiple operators used to obtain the data. Standards for timber analysis suggest the use of reference values, however these values do not exist for bamboo properties. The generally accepted method for assessing bamboo data is to compare obtained values with published data. Table 8 presents values of average tensile modulus of elasticity and shear modulus for the six segments of analysis and their standard deviation (s).

segment	Shear modulus [MPa]				Modulus of elasticity [MPa]			
	n	$\bar{x}$	s	% s of $\bar{x}$	n	$\bar{x}$	s	% s of $\bar{x}$
BI	3	79,84	26,94	34%	3	7470,00	1313,80	18%
MI	3	60,75	48,35	80%	3	16278,53	6714,67	41%
TI	3	42,27	10,90	26%	3	12061,03	8263,40	69%
BO	3	75,83	23,99	32%	3	7853,83	3315,94	42%
MO	3	105,55	5,10	5%	3	16168,33	7144,57	44%
TO	3	52,20	27,19	52%	3	18385,67	11872,36	65%

Table 8 Tensile modulus of elasticity E_t and shear modulus G of test specimens.

Standard deviation values as a percentage of averages show the high variability between samples, which ranges from 5% to 80%. This variability can be attributed to multiple sources, but is often a result of the material itself. However, the limited number of tests for each segment tends to increase the range of variability. This variability can be seen graphically on Figures 35 and 36 where modulus values are plotted with respect to longitudinal location, inner wall results are located over outer wall ones, to help visualizations the differences. However, those ranges show some trend in terms of longitudinal and wall divisions.

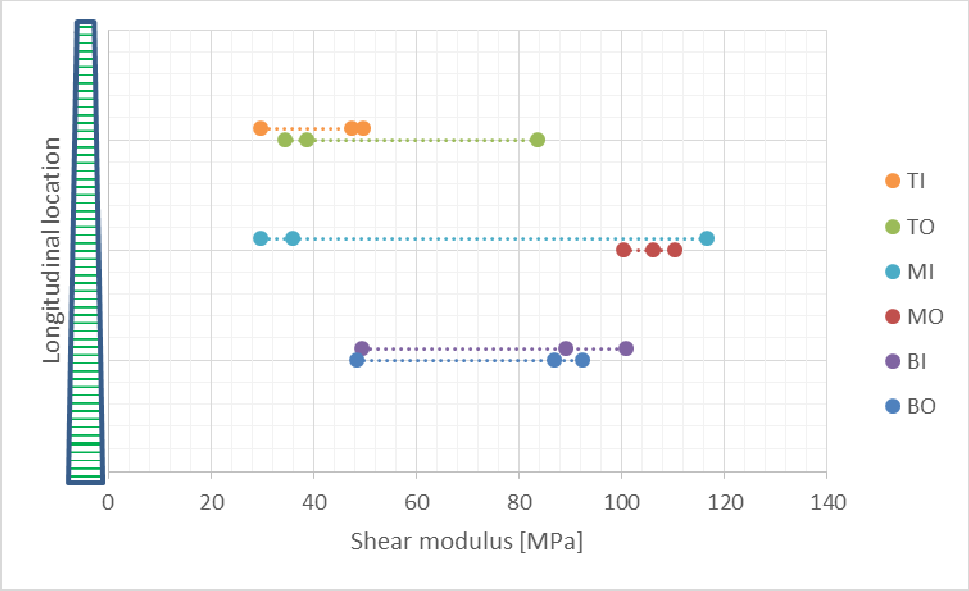

Figure 34 Shear modulus of inner and outer walls vs longitudinal location.

While Figure 35 presents an apparent random distribution of shear modulus both for longitudinal and radial location, Figure 26 presents a slight tendency to increase MOE as it goes from bottom to top.

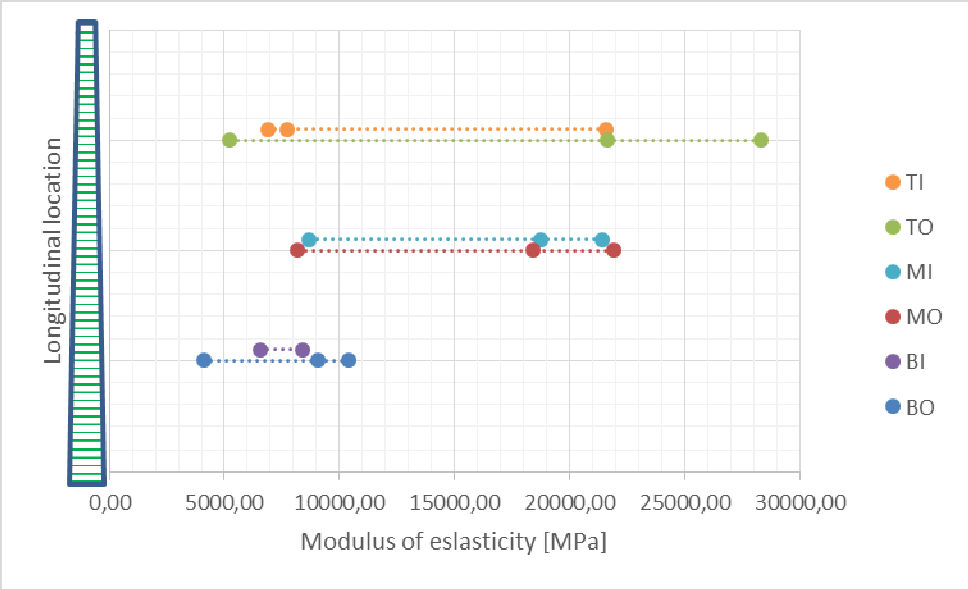

Figure 35 Tensile modulus of elasticity of inner and outer walls vs longitudinal location.

The standard deviation of the modulus of elasticity confirms wide variability resulting from heterogeneous and orthotropic materials as bamboo. In addition, the few numbers of trials of each segment makes it impossible to determine outlier spots as random errors. While Verma & Chariar, 2012 concluded that MOE increases from inner wall outwards and from bottom to the top. For this bamboo species and test there is only a marked trend of increasing from bottom to middle segment. And a soft trend of increasing from inner to outer region. Opposite to their conclusions, inner top segment resulted to have a minor MOE than both middle segments but it was the region where the increasing from inner outwards was more visible.

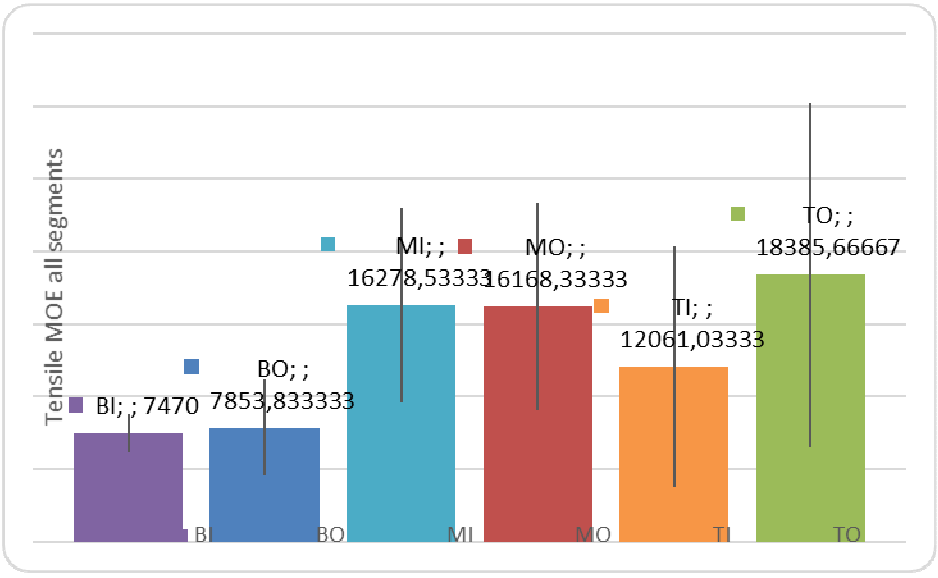

Figure 36 Tensile modulus of elasticity found for all segments of analysis.

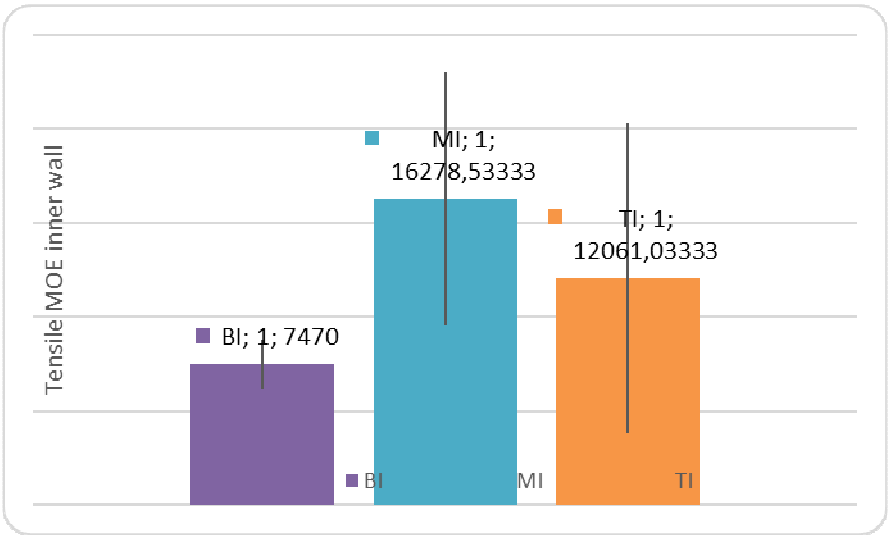

Figure 37 Tensile modulus of elasticity of inner segments.

It turns necessary to analyze inner and outer wall segments separately in order to determine some behavior patterns for individual segments. Figures 38 and 39 present tensile modulus of elasticity for inner and outer wall respectively.

A separate analysis of inner wall segments indicates a top strength for middle sections, moreover, outer wall segments show an increasing trend as some literature has suggested for some bamboo species. Addressing inner and outer regions separately, it can be said that outer regions support Verma & Chariar findings, while inner region states middle region as the higher stiffness one.

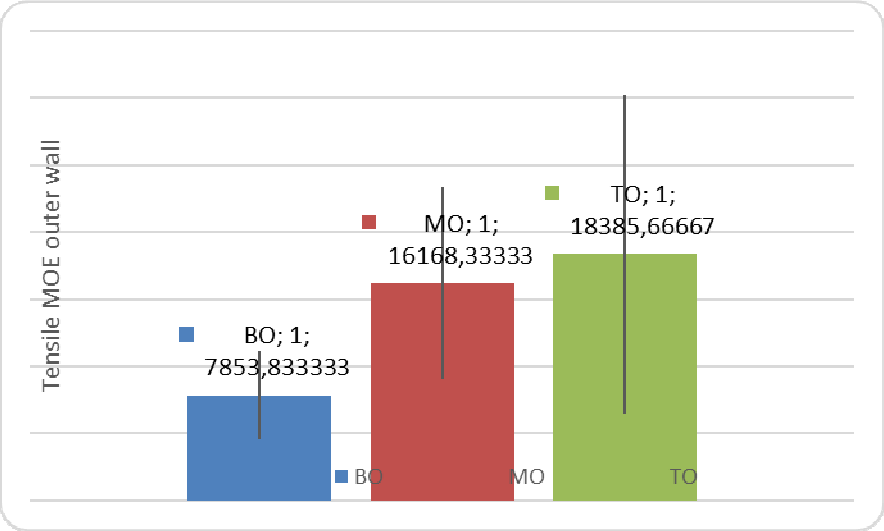

Figure 38 Tensile modulus of elasticity of outer segments.

Figure 40 and Figure 41 plot average values and the variance along the length and across the wall. Figure 40 establishes a clear trend in bottom segments compared to middle and top ones, confirming previous investigations, which established that bamboo bottom was the weakest section. However, for the middle and the top it cannot determine a defined trend, as the middle sections appears to have higher modulus than top.

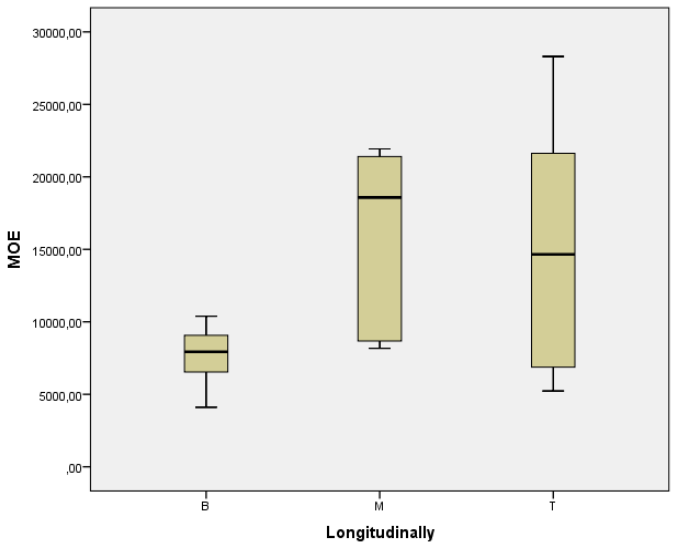

Figure 39 Marginal values of tensile MOE of segments along the length.

For marginal values of inner and outer sections on Figure 41, do not allow to determine a strong pattern across the wall thickness. However, it can be seen that outer segments seem to have higher values of MOE.

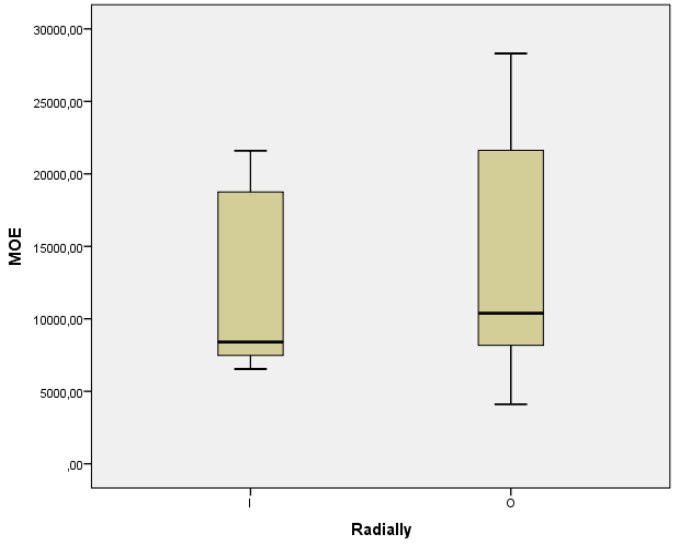

Figure 40 Marginal values of tensile MOE on wall thickness.

Previous studies encompassed bamboo culm analysis based on divisions along the culm and across the wall let to compare obtained values with relatives of other bamboo species (see Table 9). Both Verma & Chariar, 2012 and Li, 2004 found increasing values from bottom to top and from inner to outer wall for elastic constants. However, values for top sections obtained in this research do not correspond to those of literature as middle sections presented higher elastic constants.

Bamboo Et and E_b along the culm [Gpa]					
Across the wall thickness	Source	Bamboo species	Along the length		
			Bottom	Middle	Top
Inner	E_t Obando & Ghavami 2015	Dendrocalamus giganteus	7,47	16,28	7,30
	E_b Obando & Ghavami 2015	Dendrocalamus giganteus	NA	11,11	4,71
	E_t Verma & Chariar 2013	Dendrocalamus strictus	2,10	2,70	4,66
	E_b Li 2004	Phyllostachys pubescens	9,17	9,25	9,52
Outer	E_t Obando & Ghavami 2015	Dendrocalamus giganteus	7,85	16,17	18,39
	E_b Obando & Ghavami 2015	Dendrocalamus giganteus	4,70	9,32	8,29
	E_t Verma & Chariar 2013	Dendrocalamus strictus	4,60	6,40	8,90
	E_b Li 2004	Phyllostachys pubescens	16,32	16,40	16,68

Table 9 Bamboo tensile modulus of elasticity E_t and bending modulus of elasticity E_b of different culm segments for different species.

4.4.1. Statistical analysis of test specimen results

Data analysis demands determining statistical differences to classify and analyzing results. Due to high degree of dispersion of data comes highly probably do nor determine those differences, however, analysis let to generate marginal values as average values with confidence intervals based on variances so that ANOVA analysis was made for both test specimens and beam specimens. In this case, an ANOVA model for fixed effect is ineffective because longitudinal and radial position of segments turn out to be two different and independent factors, at least in this case of study. Therefore, it becomes necessary an ANOVA model of factorial design for two independent factors, in order to study the effect of each one of them for each trial. This methodology analyzes the effect along the culm and across the wall location on the response variable independently. It also provides objective results to determine if there is a choice at factor longitudinal location, which, independently of radial location, generates a better response, and vice versa. Finally, this statistical method determines what combination of both factors provides a better response, in this case, which one has better strength performance.

In a factorial design facts, as well as interaction between them are equally important for analysis. It leads to proof some hypothesis to validate ANOVA analysis:

1. Equality of the effects on longitudinal location treatment.
2. Equality of the effects on radial location treatment
3. Interaction between longitudinal and radial locations.

In this way, the first hypothesis of homoscedasticity can be accepted or rejected by using the Levene proof, which determines if variance of error remains constant along the cases. Table 10 presents Levene contrast for equality of the error variances, with longitudinal location as dependent variable. Sig. value is 0,000 therefore it is less than the significance level α=0,05. This rejects the null hypothesis and then the assumption of homoscedasticity is unsatisfied. However, for radial location the Sig. value is higher than significance level, therefore, null hypothesis is accepted and the assumption of homoscedasticity is satisfied.

MOE

Estadístico de Levene	df1	df2	Sig.
15,413	2	15	,000

Table 10 Homogeneity of variances proof for longitudinal segments as dependent variable.

MOE

Estadístico de Levene	df1	df2	Sig.
1,634	1	16	,219

Table 11 Homogeneity of variances for cross section segments as dependent variable.

Summarizes, this means that values of MOE on wall thickness measured maintain the error of the variance and on the other hand, values along the length do not. It can be seen in Figure 38 above where inner profile reaches it maximum value on middle segment and outer Figure 39, reaches it on top segment. Normality assumption should be rectified by Shapiro-Wilk proof. Table 12 shows Sig. values of 0,365 and 0,830 therefore the null hypothesis of data, which states that it comes from a normal distribution, is accepted and normality assumption is satisfied too. In other words, this indicates that values present a normal distribution.

	Kolmogorov-Smirnov[a]			Shapiro-Wilk		
	Estadístico	gl	Sig.	Estadístico	gl	Sig.
Residuo para MOE	,157	18	,200*	,946	18	,365
Residuo para MOE	,116	18	,200*	,972	18	,830

*. Esto es un límite inferior de la significación verdadera.

a. Corrección de significación de Lilliefors

Table 12 Normality proof.

Finally, the residue graph Figure in 42 was generated. This Figure analyzes intersections of residue vs observed values, identifying some linear or defined pattern. The absence of any pattern shows independence, and allows accepting the assumption.

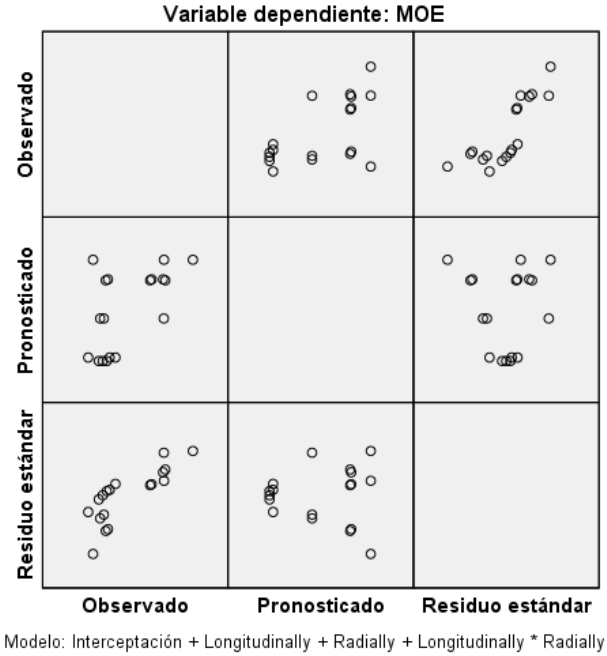

Figure 41 Residue graph.

After verifying the required assumptions, the ANOVA analysis allows concluding about the existence of significant differences between segments of analysis. However, the Sig. values on Table 13 for longitudinal and wall location are 0,187 and 0,567. Those values are higher than the significance level (α=0,05), therefore null hypothesis cannot be rejected and it can be stated objectively that there are significant differences. Nevertheless, it provides evidence that shows

that longitudinal segments vary less than wall division segments. Although it is possible to determine an objective difference between groups, a 0,187 Sig. value allows to assume a closeness to significance level 0,05.

Variable dependiente: MOE

Origen	Tipo III de suma de cuadrados	gl	Cuadrático promedio	F	Sig.
Modelo corregido	290385225[a]	5	58077044,97	1,007	,458
Interceptación	2823674614	1	2823674614	48,956	,000
Longitudinally	225814371,5	2	112907185,7	1,958	,187
Radially	20094056,77	1	20094056,77	,348	,567
Longitudinally * Radially	37412581,55	2	18706290,77	,324	,730
Error	634453459,6	11	57677587,24		
Total	3960824096	17			
Total corregido	924838684,4	16			

a. R al cuadrado = ,314 (R al cuadrado ajustada = ,002)

Table 13 Inter-subjected effects proof ANOVA table.

On the ANOVA table it can be determine the optimal statistic method for analyzing data by comparing average quadratic errors from longitudinal and cross sectional divisions. If quadratic average error is less than quadratic errors of factors (longitudinal and cross sectional), a factorial design analysis by blocks can be carried out. In this case, longitudinal level presented a better performance that can be grouped, even when no level presented significant differences.

MOE

	Longitudinally	N	Subconjunto 1
HSD Tukey[a,b,c]	B	5	7700,3000
	T	6	15223,3500
	M	6	16223,4333
	Sig.		,190

Se visualizan las medias para los grupos en los subconjuntos homogéneos.
Se basa en las medias observadas.
El término de error es la media cuadrática(Error) = 57677587,238.

a. Utiliza el tamaño de la muestra de la media armónica = 5,625.

b. Los tamaños de grupo no son iguales. Se utiliza la media armónica de los tamaños de grupo. Los niveles de error de tipo I no están garantizados.

c. Alfa = 0,05.

Table 14 HSD Turkey table.

According to HSD Turkey analysis, longitudinal location levels are similar, despite of visible difference of values at first glance. However, there is a relevant fact in Table 14 that indicates a higher MOE value for middle segments. Table 15 shows a statistical analysis of relationships of each level with others. On the Sig. values it can be seen the trend of M as the highest section, and the close relationship between middle and top, and the trend to decrease values of B sections.

Comparaciones múltiples

Variable dependiente: MOE

	(I) Longitudinally	(J) Longitudinally	Diferencia de medias (I-J)	Error estándar	Sig.	Intervalo de confianza al 95% Límite inferior	Límite superior
HSD Tukey	B	M	-8523,1333	4598,74425	,198	-20943,6829	3897,4162
		T	-7523,0500	4598,74425	,272	-19943,5995	4897,4995
	M	B	8523,1333	4598,74425	,198	-3897,4162	20943,6829
		T	1000,0833	4384,73060	,972	-10842,4460	12842,6127
	T	B	7523,0500	4598,74425	,272	-4897,4995	19943,5995
		M	-1000,0833	4384,73060	,972	-12842,6127	10842,4460
DMS	B	M	-8523,1333	4598,74425	,091	-18644,9012	1598,6345
		T	-7523,0500	4598,74425	,130	-17644,8178	2598,7178
	M	B	8523,1333	4598,74425	,091	-1598,6345	18644,9012
		T	1000,0833	4384,73060	,824	-8650,6436	10650,8103
	T	B	7523,0500	4598,74425	,130	-2598,7178	17644,8178
		M	-1000,0833	4384,73060	,824	-10650,8103	8650,6436

Se basa en las medias observadas.
El término de error es la media cuadrática(Error) = 57677587,238.

Table 15 multiple segments comparison by HDS Turkey and DMS.

Statistical analysis provides marginal MOE values for both along the length and wall thickness. Figure 43 plots MOE marginal averages for longitudinal segments. It presents a clear sameness between inner and outer MOE of bottom and middle sections, rising from bottom upwards. However, for the top section it results in different values for inner and outer parts, being outer one higher than middle average and the inner one lower.

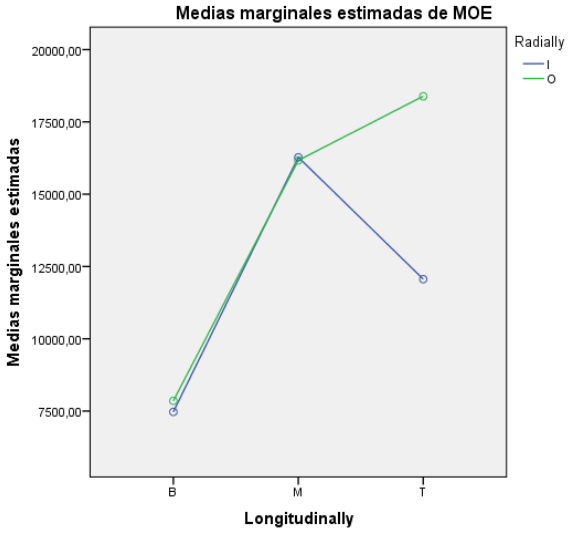

Figure 42 Estimated marginal averages of MOE along the length.

On the other hand, marginal measures along the wall thickness evidence small differences between inner and outer parts for bottom and middle sections. In addition, it marks a defined rising trend for the top segment from inner outwards.

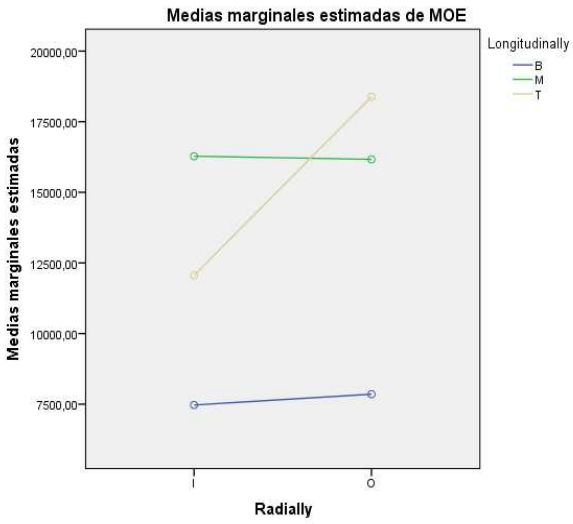

Figure 43 Estimated marginal averages of MOE along the wall thickness.

4.5.
Beam analysis

Bending test provides numerous ways to obtain mechanical properties of materials and beams as well. Available methodologies generate results, which depending on what it is being measured, turn out to be the suitable or not. In this case, four different ways to obtain modulus of elasticity were used and the results are presented on Table 16. Those results are compared with control data, tensile modulus of elasticity, obtained in order to determine any pattern on behavior of segments of analysis and beams.

Displacement modulus of elasticity was obtained by solving the integration method, for beam analysis of mechanical of materials using LVDT readings. Strain modulus of elasticity was calculated by strain gage readings located at the upper and lower surface of beam mid-span. Apparent modulus and shear corrected were obtained using formulas suggested by ASTM D198 for statics tests of lumber in structural sizes. Data for segment Bottom-Inner BI was lost due to fails on the acquisition system. Consequently, lack of information hinders any analysis involving this segment.

Bending Modulus of elasticity acquisitions		segment					
		BI	MI	TI	BO	MO	TO
Tensile Modulus of elasticity MPa	n	3	3	3	3	3	3
	$\bar{x}$	7470,00	16278,53	12061,03	7853,83	16168,33	18385,67
	s	1313,80	6714,67	8263,40	3315,94	7144,57	11872,36
	% s of $\bar{x}$ control	18%	41%	69%	42%	44%	65%
Displacement Modulus of elasticity MPa	n	0	3	3	3	3	3
	$\bar{x}$	NA	11109,00	4708,33	4698,00	9317,00	8287,00
	s	NA	2752,93	182,56	795,56	3959,16	548,34
	% s of $\bar{x}$	NA	25%	4%	17%	42%	7%
	r	NA	0,85	-0,99	0,99	0,94	-0,83
Strain Modulus of elasticity MPa	n	0	3	3	3	3	3
	$\bar{x}$	NA	31388,00	13583,00	40681,33	822858,00	245302,67
	s	NA	3330,27	1962,39	37527,17	780949,68	263598,94
	% s of $\bar{x}$	NA	11%	14%	92%	95%	107%
	r	NA	0,49	-0,65	-0,94	0,97	-0,87
Apparent Modulus of elasticity MPa	n	0	3	3	3	3	3
	$\bar{x}$	NA	19887,40	6465,75	5216,88	12881,08	9710,54
	s	NA	7465,66	1231,93	464,44	3005,88	1128,70
	% s of $\bar{x}$	NA	38%	19%	9%	23%	12%
	r	NA	0,30	-0,98	1,00	0,68	0,58
Shear corrected Modulus of elasticity MPa	n	0	3,00	3,00	3,00	3,00	3,00
	$\bar{x}$	NA	1936,58	1318,48	2395,20	3188,40	1845,05
	s	NA	107,51	78,56	194,83	550,14	331,03
	% s of $\bar{x}$	NA	6%	6%	8%	17%	18%
	r	NA	0,92	-0,81	-0,95	-0,99	-0,82

Table 16 Bending modulus of elasticity obtained by four different methodologies.

Strain modulus of elasticity presented several outliers values. This could be due to random and procedure errors caused by issues relative to the data acquisition system, strain gage operation and surface characteristics. Therefore, Table 17 presents averages of *r* values in order to select suitable data for analysis. Thus, Table 15 confirm assumptions that strain modulus should be discarded. Moreover, shear corrected modulus has values substantially small compared to others. This may be due to the shear values experimentally obtained, which affect the corrected value and differences between standard lumber used and bamboo.

	Displacement Modulus of elasticity MPa	Strain Modulus of elasticity MPa	Apparent Modulus of elasticity MPa	Shear corrected Modulus of elasticity
r averages	0,19	-0,20	0,32	-0,53

Table 17 *r* averages for modulus of elasticity regarding tensile modulus.

Coefficient *r* of correlation describes similarity between two data groups, when it is close to one, both data groups are more correlated. However, both the apparent and the displacement methods are considerably far from one, but are closer than the shear corrected and strain modulus. Figures 45 and Figure 46 show longitudinal and wall profiles in order to compare graphically different modulus methodologies and then choose suitable data groups to carry out statistical analysis.

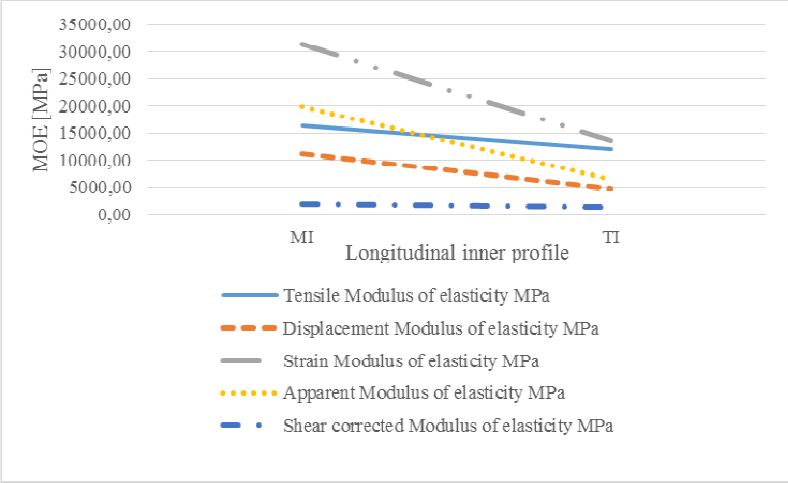

Figure 44 Longitudinal inner profile vs modulus of elasticity.

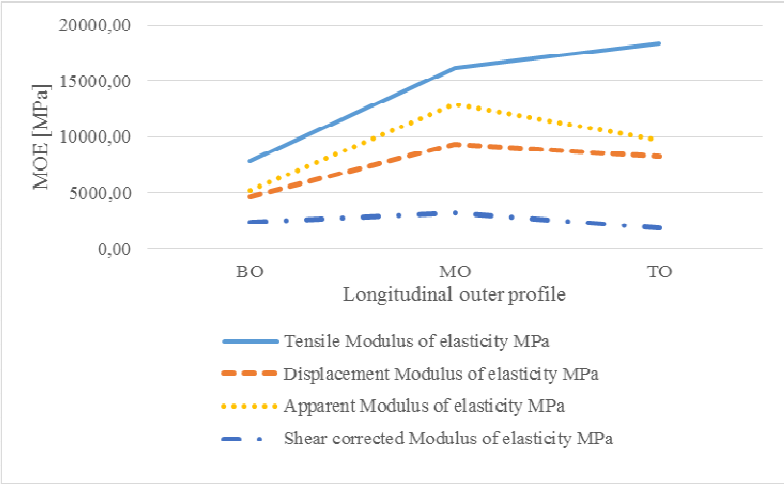

Figure 45 Longitudinal outer profile vs modulus of elasticity.

Figure 45 and Figure 46 show the displacement and apparent modulus as the curves that better fit to tensile modulus of elasticity.

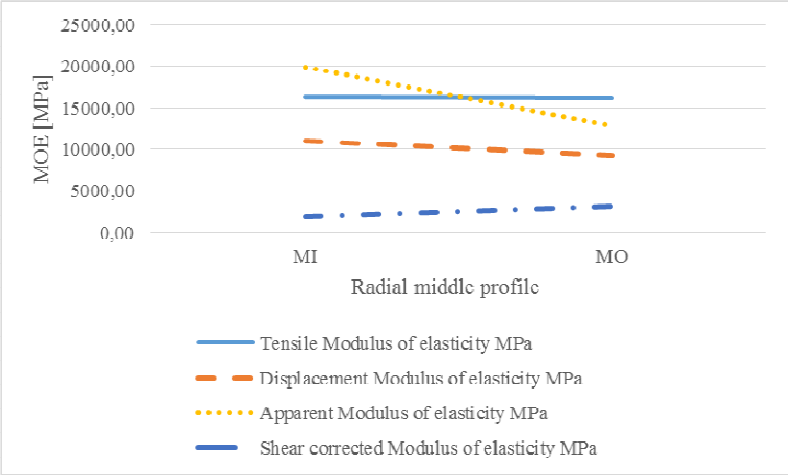

Figure 46 Wall thickness profile of middle section vs modulus of elasticity.

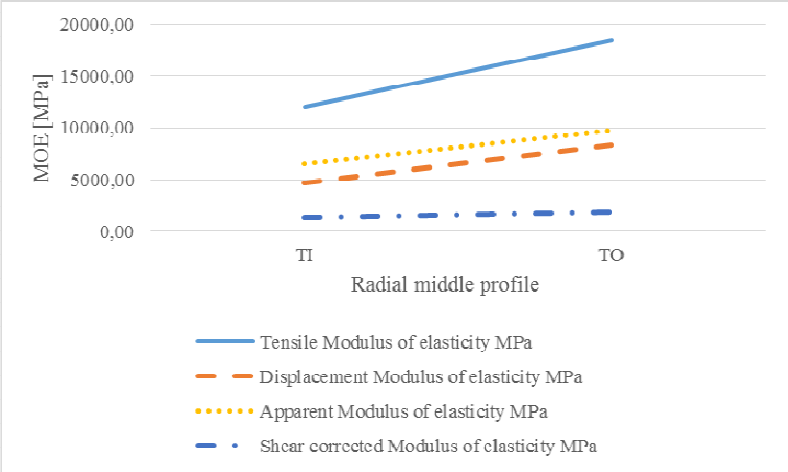

Figure 47 Wall thickness profile of top section vs modulus of elasticity.

4.5.1. Statistics bending data analysis

To compare experimental tensile modulus with displacement and apparent modulus it is necessary to carry out another statistic analysis as variability and heterogeneity are strictly linked to the results of the response variable. Therefore, it should be determined if the difference between the two experimental units subjected to different treatments (method of modulus acquisition), is due to a real difference between treatment effects or due to heterogeneity of samples. Randomized block design is the method used for this statistical analysis.

Segments of analysis compose blocks, and the treatments are assigned randomly to the blocks. This design strategy improves accuracy when compared to reducing residual variability. All treatments run into each block, which implies a restriction over randomization.

Levene proof verifies variances equality. Sig. value in this case is 0,04, as shown in Table 18, which is close to a significance level of 0,05. This rejects homoscedasticity assumption and the null hypothesis, however, for further analysis the low range of difference between Sig. value and significance level could be determinant. Despite Sig. value rejects hypothesis, it is very close to significance value, even more in the case of anisotropic materials analysis.

Variable dependiente: MOE

F	df1	df2	Sig.
2,138	14	30	,040

Prueba la hipótesis nula que la varianza de error de la variable dependiente es igual entre grupos.

a. Diseño : Interceptación + segment + method

Table 18 Equality Levene proof of error variances.

Normality verification of data requires Shapiro-Wilk proof. For this proof all Sig. values in Table 19 are higher than 0,05 except for the TI. Therefore, it can be said that normality assumption is met for most of the segments of analysis, except for TI segment.

Pruebas de normalidad

		Kolmogorov-Smirnov[a]			Shapiro-Wilk		
	segment	Estadístico	gl	Sig.	Estadístico	gl	Sig.
Residuo para MOE	MI	,238	9	,151	,901	9	,255
	TI	,357	9	,002	,746	9	,005
	BO	,197	9	,200*	,892	9	,208
	MO	,149	9	,200*	,960	9	,796
	TO	,290	9	,028	,902	9	,263

*. Esto es un límite inferior de la significación verdadera.

a. Corrección de significación de Lilliefors

Table 19 Normality proof.

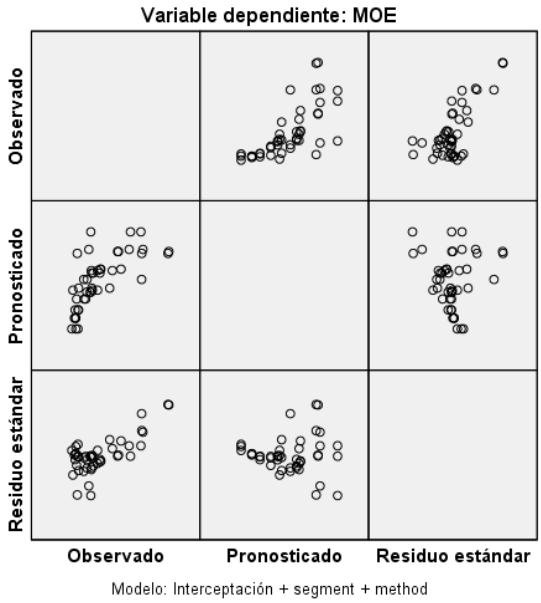

Figure 48 Square residual for beam data analysis.

The independence assumption is verified by identifying some defined patterns at square residual vs prediction as shown in Figure 49. At first glance, there are not any patterns so the assumption is accepted.

Variable dependiente: MOE

Origen	Tipo III de suma de cuadrados	gl	Cuadrático promedio	F	Sig.
Modelo corregido	890003419,822[a]	6	148333903,304	5,814	,000
Interceptación	5315647493,889	1	5315647493,889	208,354	,000
segment	570591349,111	4	142647837,278	5,591	,001
method	319412070,711	2	159706035,356	6,260	,004
Error	969478947,289	38	25512603,876		
Total	7175129861,000	45			
Total corregido	1859482367,111	44			

a. R al cuadrado = ,479 (R al cuadrado ajustada = ,396)

Table 20 Inter-subjects effects proof ANOVA table.

Differences between methods were clear since r coefficient averages were between 0,19 and 0,32 (displacement and apparent), regarding the tensile modulus. Moreover, according to ANOVA results in Table 20 there are significant differences among segments too. Sig. values are between 0,001 and 0,004 both lower than significance level 0,05.

Table 21 presents averages values and limits for each segment of analysis, and Figure 50 shows them graphically. Those limits confirm the difference between segments and put forward middle segment as the strongest of all.

1. segment

Variable dependiente: MOE

segment	Media	Error estándar	Intervalo de confianza al 95%	
			Límite inferior	Límite superior
MI	15758,333	1683,667	12349,928	19166,738
TI	7745,000	1683,667	4336,595	11153,405
BO	5922,889	1683,667	2514,484	9331,294
MO	12788,778	1683,667	9380,373	16197,183
TO	12127,778	1683,667	8719,373	15536,183

Table 21 MOE averages for segments.

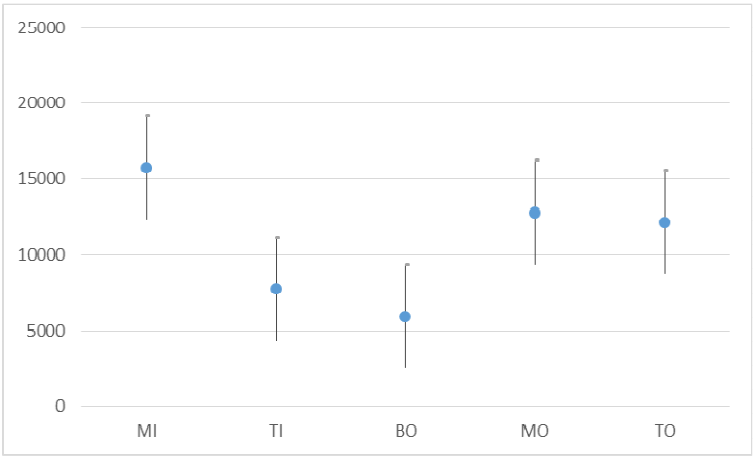

Figure 49 Limits of average MOE for segments.

When comparing both experimental and more accurate methods for obtaining modulus with tensile test, it can be said that all three methods fit on a range relatively thin regarding difference between specimens and beams, experimental and random errors and number of trials. Estimated marginal values

for MOE in Figure 51 defines middle section as strongest section, and presents an evident fall from middle to top. Bottom section remains as the one with the lowest values.

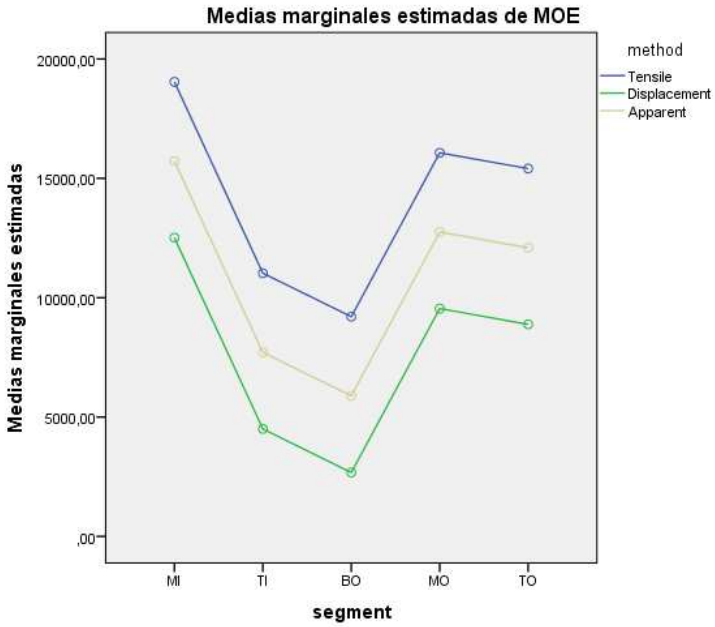

Figure 50 Estimated marginal averages of MOE for segments of analysis

4.6. Failure analysis

ASTM D143 – 14 for specimens of timber, explains the types of failure in static bending, as it was presented in the second chapter. However, in terms of fracture surfaces, bamboo may be roughly divided into brash and fibrous. The term brash indicates abrupt failure and fibrous indicates a fracture showing splinters. Moisture content is an essential factor to determine the type of fracture.

Table 22 shows types of failure of each laminated bamboo beam. Moreover, it presents an alternative secondary cause of failure, related to failures that preceded the initial fracture during the tests. Another classification in terms of surface fracture is included as well. The results presented a marked trend to fibrous surface fracture on the inner specimens and brash surface fracture for outer ones. Inner specimens failed due to tensions strengths considered simple, splintering and brash tension with a great presence of horizontal shear and inner compression strengths as secondary causes of failure. Outer specimens presented a

predominant horizontal shear and brash tension as primary cause of failure, and compression with horizontal strengths as secondary cause for inner specimens.

	Specimen	Primary type of failure	Secondary type of failure	Surface fracture
1	BI	simple tension	horizontal shear	fibrous
2	BI	simple tension	horizontal shear	fibrous
3	BI	splintering tension	horizontal shear	fibrous
4	MI	splintering tension	inner compression	fibrous
5	MI	splintering tension	inner compression	fibrous
6	MI	splintering tension	inner compression	fibrous
7	TI	simple tension	inner compression	brash
8	TI	simple tension	inner compression	brash
9	TI	brash tension	inner compression	brash
10	BO	horizontal shear	compression	fibrous
11	BO	horizontal shear	compression	fibrous
12	BO	brash tension	horizontal shear	brash
13	MO	horizontal shear	compression	brash
14	MO	horizontal shear	compression	brash
15	MO	horizontal shear	compression	brash
16	TO	brash tension	horizontal shear	brash
17	TO	brash tension	inner compression	brash
18	TO	brash tension	inner compression	fibrous

Table 22 Types of primary and secondary failures on the beams and surface fracture.

Figures below show different type of fracture on beam specimens.

Figure 51 Fracture on beam specimen 3 by splintering tension and horizontal shear.

Figure 52 fracture on specimen 17 by brash tension and inner compression.

Figure 53 Fracture on specimen 8 by simple tension and inner compression.